DYNAMIC POSITIONING CONFERENCE
September 18-19, 2001

HIGH TECH SESSION

"What Happens in Water"

The use of Hydrodynamics to Improve DP

Radboud R. Th. Van Dijk and Albert B. Aalbers
Maritime Research Institute Netherlands (Wageningen)

1. Introduction

For dynamic positioning the most important factors determining the positioning capability are carried through the water. The thrusters act in water to generate the forces needed to keep on station and the waves and current cause – besides wind - the major forces pushing the vessel off station.

Hydrodynamic research has been carried out to quantify the effectivity of a thruster in model scale operational conditions. It shows that degradation effects may occur due to inflow and cross flow, and due to waves if this causes ventilation effects. Other investigations show that the water accelerated by the thruster may have effect on other hull parts so that the net force generated is less than expected. In the paper examples of such degradation effects will be shown
As excitations, the wave drift forces acting on the vessel may be of significant magnitude. Incorporating a real time estimate of these forces in the DP control system allows improved DP, similar to what has been obtained by wind feed forward. In the paper a method will be described for such real time estimating, and results will be presented of application of wave feed forward on model scale.

The application of the hydrodynamic information is useful for the large deep water DP drilling rigs, ship shape or semi-submersible, extending their operational limits and saving fuel cost.

Acknowledgement

The Authors would like to thank the companies Petrobras, Diamond Drilling and Santa Fé Drilling for their cooperation by allowing us to use model test results for this paper, thereby greatly enhancing the value of the presentation.

2. Thrust degradation effects

2.1 Thruster performance

All thrust generators work on the principle of accelerating water. So, there is a suction side flow and a jet flow. The suction flow is characterized by relatively low flow velocity over a wide area, while the jet flow is high speed and concentrated in a relatively small cross section. Furthermore, the jet may induce other flow patterns, depending on the local hull form and the intensity and direction of the jet. These flows, together with current flow and waves may cause interaction effects leading to degradation of thruster performance. Generally the following types of interaction are considered:

- Thruster-thruster
- Thruster-hull
- Thruster-current
- Thruster-waves

2.2 Interaction effects

Thruster-thruster interaction

Thruster-thruster interaction always leads to thrust degradation, and the main causes are listed below.

- Forces due to blockage, when the jet of one thruster hits another thruster.
- Thruster efficiency loss, when the jet of one thruster interferes with the suction flow of the other thruster.

Usually these effects occur simultaneously. The effects have been well described and studies, e.g. by Nienhuis (Ref. 1) and Minsaas & Lehn (Ref. 2) give ample engineering information. Thruster-thruster interaction will occur between all types of thrusters and typical results for azimuthing thrusters are given in Fig. 1, from Nienhuis (Ref.1), showing significant losses.
A special case is the use of (high lift) rudders in combination with (twin) main propulsion. The longitudinal force component on the main screw is counteracted by reverse thrust on other units (e.g. the other main screw) or by longitudinal force on the rudder. The highly deflected or reverse flows may induce degradation of other units and significant hull interference effects.

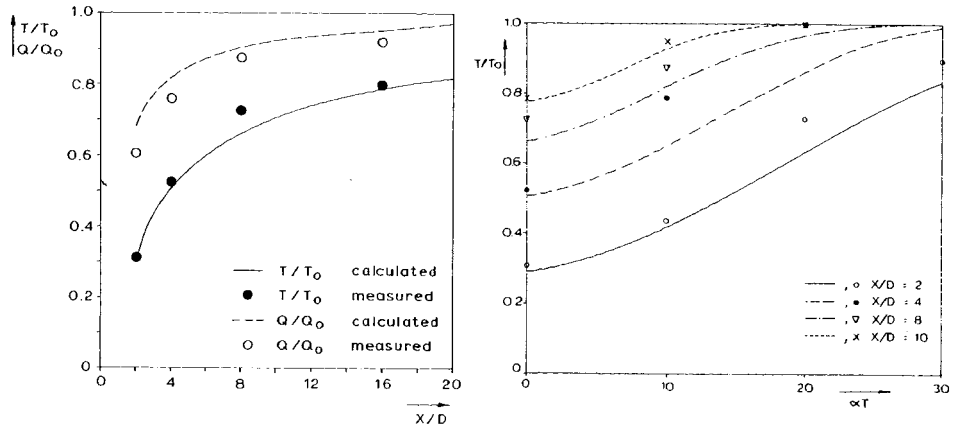

Fig.1: Thruster-thruster degradation as function of distance and azimuth angle

The most logical way to minimize thruster-thruster degradation effects is by avoiding that the jet of one thruster gets close to another thruster. Thereto forbidden sectors are specified in the thrust allocation algorithms of the DP control system.

Thruster- hull interaction

Thruster hull interaction may lead to enhanced as well as decreased performance of the thrust unit. The basic effects are:

- Fricion losses of the jet flow with the keel of the vessel
- Induced pressures on the hull due to Bernoulli's dynamic pressure term ($-{}^1/_2\rho v^2$).
- Forces due to blockage when the jet hits a structural element, such as a skeg.

On a large hull the friction losses can be significant. For tunnel thrusters the induced pressures may generate a significant additional force if there is no current or forward speed, see Brigg (Ref. 3) and Nienhuis (Ref. 1).
For azimuthing thrusters, e.g. below a semi submersible pontoon, a strong interaction effect may occur if it is turned in transverse direction. The thruster wake is deflected upwards, due to the Coanda effect and causes a low-pressure region next to the pontoon. The deflection of the wake depends on the shape of the pontoon and the bilge radius, as well as on the distance between the thruster and the bilge as shown in Figure 2, (Nienhuis, Ref. 1). It will lead to a reduction in the delivered thrust. Also, the Coanda effect can result in a further increase of the thrust loss due to the impact of the jet on the opposite pontoon of a semi-submersible. A downward angle of the propeller shaft, as is often applied, will reduce both the suction effect and the blockage effect.

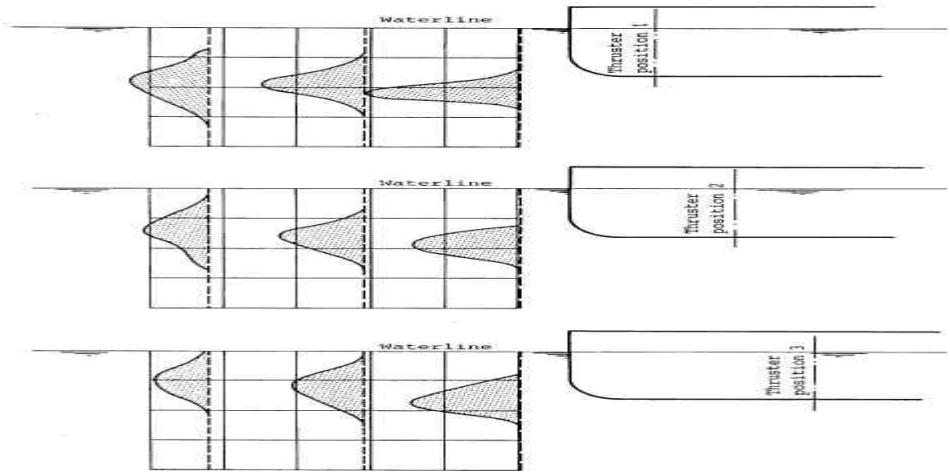

Fig. 2: Jet flow of a thruster under a round bilge hull.

Figure 3 [a] and [b] show an azimuthing thruster at the bow resp. stern of a semi submersible starboard pontoon. The vector indicates the thrust direction of the azimuthing thruster. At the origin of the vector the delivered total thrust force can be found as a percentage of the open water thrust in bollard pull condition. The solid line shows the resulting total thrust force without current. This line clearly shows the above mentioned thruster-thruster interaction effects.

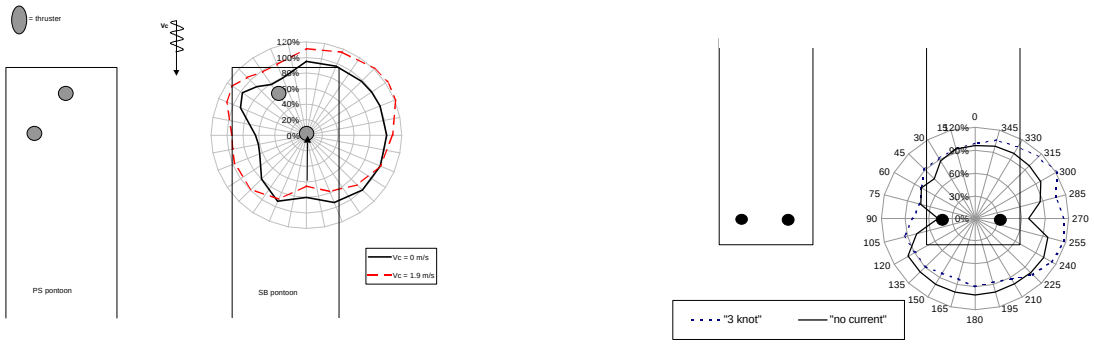

Fig. 3 [a] and [b]: Thruster degradation effect on two different semi-submersibles:
a) Of single bow thruster (Courtesy Petrobras)
b) Of two stern thrusters combined (Courtesy Santa Fé Drilling)

At an azimuth angle of about 0 degrees (Fig. 3[a]) and about 180 degrees (Fig. 3[b]) the resulting thrust force is degraded due to friction forces between the jet flow and the pontoon bottom. For both semis the azimuthing thruster shaft was inclined downward at 5 degree. In Fig. 3[b] the bow thruster units were not present in the model. This leads to lower degradation effect (absence of blockage of jet flow by inactive thruster).
At azimuth angles with the jet flow towards the other pontoon, the total delivered thrust force is significantly reduced.

Thruster-current interaction

Current, together with the flow past the hull due to the drift motions of the vessel, leads to two effects:

- Direct performance interaction due to inflow
- Modification of the thruster-hull interaction effects, due to changes in flow directions and pressure fields

The first effect can be evaluated with performance diagrams. The performance of a ducted azimuthing thruster unit can be measured for a range of azimuth angles è and a relative (current) velocity V_{rel}. The vector T indicates the unit thrust. The dimensionless advance coefficient J and thrust coefficient K_T of the thruster are defined as follows.

$$J = \frac{V_{rel}}{n \cdot D_{thr}} \qquad (1)$$

$$K_T = \frac{T}{\tilde{n}_{water} \cdot n^2 \cdot D_{thr}^4} \qquad (2)$$

In the Figure 4 from Cozijn et al (Ref. 4), the K_T-J curves have been plotted. The K_T-J curves show a number of things about the behavior of the thruster in current.

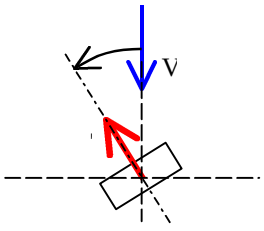

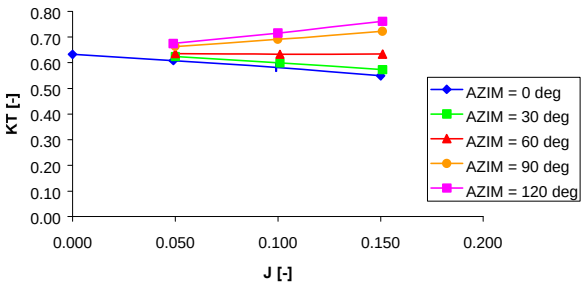

Fig. 4: Efficiency curves for a thruster

At azimuth angles between 0 and 60 degrees (0 degrees = thrust vector T directed into the current) and constant RPMs the unit thrust T will decrease for increasing relative current velocities V_{rel}. At azimuth angles between 60 and 120 degrees and constant RPMs the unit thrust T will increase for increasing relative current velocities V_{rel}. The thrust increase is negligible for an azimuth angle of 60 degrees and can be up to 30% of the bollard pull thrust for an azimuth angle of 120 degrees.
For normal offshore conditions, this direct influence of 'current' speed is small for (azimuthing) thrusters and main propellers, since the thrust of a propeller hardly varies for the low speeds involved. For water jet thrusters it may also be assumed that the current flow over the inlet will hardly affect the unit thrust.
However, for high current conditions (e.g. the 'Loop Currents" in the Gulf of Mexico, and 'Foz do Amazonas') or during DP tracking where the forward speed may also be interpreted as a 'current', larger interaction effects may be expected. Especially azimuthing thrusters with high P/D ratio, which are optimized for still water performance, suffer from significant efficiency loss, depending on the flow direction (see Figure 5). For ships with application in such high 'current' conditions, selection of thrusters optimized at a few knots speed is preferable.

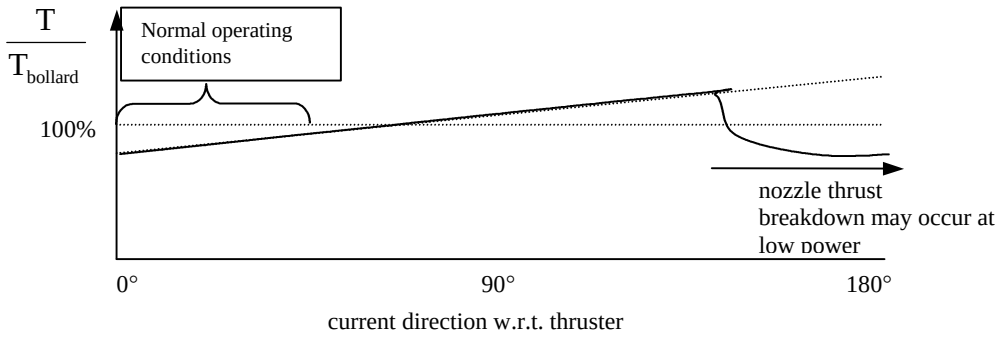

Fig 5: Schematic thruster performance in 4 kn. current

It should be noted that the change in unit thrust T at constant RPMs will be accompanied by a change in torque Q. This means that the consumed power of the thruster will also change, which phenomenon has been used to suggest thruster control on basis of power, thereby 'automatically compensating for current interaction (Deter & Shatto 1999, Ref. 5.)

In Fig. 3[a] for the semi submersible, the dashed line shows the total thrust force for the same condition with a 1.9 m/s current from the bow. The following behavior can be observed.
Due to the presence of current the delivered thrust force will decrease for an azimuth angle of 0 degrees, while it will increase for an azimuth angle of 180 degrees. This effect is caused by the change of the thruster inflow velocity, as discussed in the previous section.
For azimuth angles of 90 and 270 degrees the presence of current leads to an increase in the delivered total thrust force. The thruster-current interaction effects observed here have already been discussed in the previous section. However, for an azimuth angle of 90 degrees also another effect plays a role here. Due to the high current velocity, the thruster wake will be deflected and not reach the opposite pontoon. This reduces the thruster-hull interaction, which is clearly present without current. In Fig. 3[b] similar effects are found for the stern thrusters in a 3 kn current from the bow.

Thruster-wave interaction

There are two major effects that can be discerned:
- Degradation caused by oscillating flow due to waves
- Degradation due to ventilation

From investigations it has been demonstrated that the flow variations due to ship motions and waves at propellers under the ship can be significant. For deeply submerged thrusters these oscillating flows may cause degradation, but due to the anti-symmetric relation between K_T and J the mean degradation is small.

For tunnel thrusters, however, the wave interaction can be dramatic: if the inlet sucks air, the thrust of the unit collapses as shown in Figure 6 below. It takes significant time to build up again, depending on the length of the tunnel.

In an experimental research programme carried out at MARIN (Ref 6) a empirical simulation model was developed to predict degradation in waves. It was expected that the thrust degradation would be mainly caused by air suction of the tunnel thruster. An important parameter for air suction is the relative wave height at the tunnel entrance. The thrust degradation was found to be most significant for the following conditions:

- large wave heights.
- bow and bow quartering wave directions.
- encounter frequencies close to the ship's natural frequency for heave, pitch and roll.
- wave directions such that the wave hits the intake side of the tunnel thruster.

Within the time domain simulation program DPSIM this procedure is followed within one DPSIM time step as a separate time domain simulation with a much smaller time step. The results show a realistic drop and build-up time for the thrust, see Figure 6.

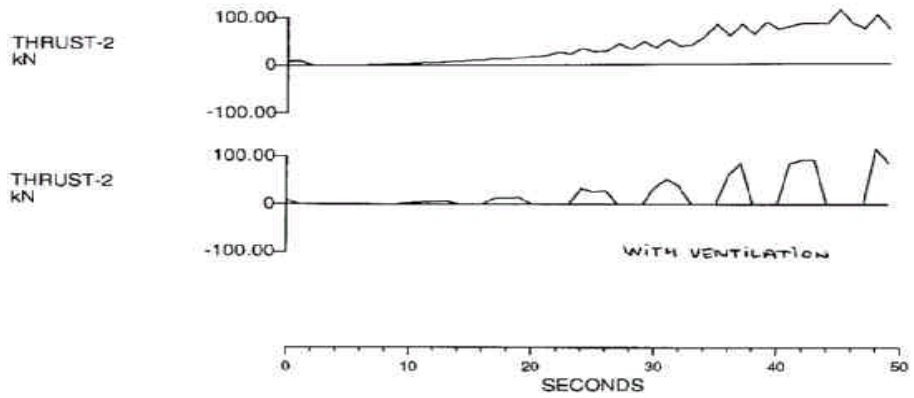

Fig. 6: Simulated bow thruster performance in a time domain DP simulation, the same phase of positioning is shown without and with ventilation due to waves

2.3 Summary

The general behavior of thrusters in degrading conditions has been investigated by means of model tests and mathematical models are available for a number of effects. This allows to generally quantify degradation effects in design stage. In thrust allocation algorithms it is possible to compensate for thruster degradation effects. However, given the effect of current on e.g. interaction effects for semi-submersibles, it is desirable to have a real time current estimate available as can be derived from the “rest force” estimator of the DP system after combining wind feed forward with wave feed forward.

3. Dynamic Positioning control using wave feed forward

3.1 Wave drift forces

The waves at sea generate a slowly varying force on a floating object (e.g. a ship) so that it drifts, even in absence of current and wind. These forces originate from second order processes in the interaction between the waves and the ship hull and have been described in detail by Pinkster (Ref. 7)
The following gives a condensed description as far as relevant for the drift force estimation in the wave feed forward methodology.

Using the fluid potential Φ, the mathematical description of the wave drift force from pressure integration techniques is

$$\overline{F} = -\tfrac{1}{2}\int_{WL} \rho g s_r^2\, n.dl + a \times (M \ddot{x}_g) - \int_S -\tfrac{1}{2}\rho |\nabla f|^2 dS - \int_S \rho (x \cdot \nabla f_t\, n)\, dS - \int \rho f_t\, n.dS \qquad (3)$$

This expression is obtained by Taylor Series expansion of the pressures and subsequent forces up to second order. The five contributions are:

- The first contribution is the drift force contribution from the relative water motion s_r around the hull, and is the most important contribution
- The second contribution is an interaction effect between the vessel's angular motions $\underline{\alpha}$ and its translational bodily accelerations $\underline{x}_g$ in the center of gravity G.
- The third contribution is from the hydrodynamic pressure in Bernoulli's Law ($p = {}^1/_2 \rho v^2$), with $\underline{v}=\nabla\Phi$
- The fourth is caused by interaction of local translations of the vessel hull in a pressure gradient, where $\Phi_t = {}^d/_{dt}\Phi$.
- The fifth contribution is due to the so-called 'set-down' waves, a strong effect in shallow water (Water depth < 0.5 wave length)

Given a wave spectrum $S_\zeta(\omega)$, the mean drift force in that spectrum can be readily derived from:

$$\overline{F} = 2\int_0^\infty T(w,w) S_z(w)\, dw \qquad (4)$$

Herein $T(\omega,\omega)$ physically represents the mean wave drift force in a regular wave with frequency ω. The magnitude of the wave drift force quadratic transfer function $T(\omega,\omega+\mu)$ can be determined from sink-source potential theory computations using the Eq. (3) in discretised frequency domain.

3.2. Wave Feed Forward: Wave drift force estimator

Two methods will be described for the estimation process of the wave drift forces in real time. The basic assumptions are respectively:
Method 1: The wave drift forces are dominated by the relative motion contribution
Method 2: The wave drift forces are in phase with the envelope of the wave groups

In both methods the wave drift forces are quantified through analysis of the relative motions along the hull. The first mentioned method, described by Pinkster (Ref. 8) requires many measurement locations around the hull of the vessel. The second approach is derived from the notion that a good estimate of the wave drift forces can be made if the wave direction with respect to the vessel is known. The method requires only three measurement locations on the bow and shoulders of the vessel (assuming that the vessel heading under DP will be more or less into the waves). The method to estimate the dominant wave direction is first described by Aalbers and Nienhuis (Ref. 9).

Method 1. Using full integration along the waterline (with 10 wave probes).

The wave drift force is estimated by numerical integration of the low pass filtered pressure from the relative motion squared along the waterline, conform the first term in Eq. (3):

$$-\frac{1}{2} r g \oint_{WL} S_r^{\,2}(x) \cdot n \cdot dx \approx F^{(2)}(t, a_{rel}) * C_f \qquad (5)$$

in which C_f is a correction factor to tune the magnitude of the total drift forces to that of the first contribution in Eq. (3).

Method 2. Based on wave direction measurement and using drift force transfer functions.

Measurement probes for the relative water motion at the side of the ship are located at the bow and at the shoulder on Port and Starboard side. The sensor at the bow is used to measure the average period T_{zus} and the "envelope squared" $A_s^2(t)$ of the relative motion at the bow. The sensors at the shoulders are used to derive the wave direction $\alpha_r(t)$. All these values: T_{zus}, $A_s^2(t)$ and $\alpha_r(t)$ are the result of averaging or low pass filtering to be applicable in the time scale of wave groups instead of individual waves.

Since these filtering or averaging processes are leading to a phase lag, the method applies the information on T_{zus}, $A_s^2(t)$ and $\alpha_r(t)$ as if it is valid for the "undisturbed' wave passing at the vessel midship. The travel time of the waves from bow to midship is approximately equal to the phase lag of the filters.

The theoretical basis of method 2 is that with standard numerical tools the mean wave drift force acting on a vessel in a given wave spectrum (with unit wave height) can be calculated as a function of the average (zero upcrossing) wave period and the wave direction. Using the wave envelope squared as modulation function, the wave drift force on the vessel can be evaluated. However, instead of the wave period and envelope, the relative motion period and envelope are measured, so it is necessary to re-write the spectral equation (Eq. (4)) for mean wave drift force as a function of the relative motion "s". The method is described in detail by Aalbers, Tap and Pinkster (Ref. 10) and makes an estimate of the instantaneous wave drift force, using the measurement of the relative motion at the bow as follows:

$$F_j^{(2)}(t) = \overline{F}_j^{(2)}(t) \frac{\left[s_{BOW}^{\,2}\right]_{LP}}{\left[\overline{s_{BOW}^{\,2}}\right]_{LP}} \quad \text{with} \qquad (6)$$

$$\overline{F}^{(2)}(t) = m_{0s} \overline{F}_*^{(2)}(T_{zus}, a_{rel}), \text{ and} \qquad (7)$$

$$\overline{F}_*^{(2)}(T_{zus}) = 2 \int_0^\infty \frac{\overline{F}^{(2)}(w)}{s_a^{\,2}} S_s^{\,*}(w, T_{zus}) dw \quad \text{which can be evaluated for } T_{zus} \text{ and } \alpha_{rel} \qquad (8)$$

Herein was used that $S_s(\omega) = m_{0s} \,.\, S_s^{\,*}$, where $S_s^{\,*}$ is a unit relative motion spectrum depending on T_{zu} (of the wave) and α_{rel}.

In Eq. (6) the low pass filtered value of the relative motions squared, i.e. $|s_{bow}^{\,2}|_{LP} = {}^1/_2 A_s^2(t)$, the envelope squared, and $s_{bow}^{\,2}|_{LP} = m_{0s(Actual)}$. Due to the difference in time period for which $A_s^2(t)$ and $m_{0s(Actual)}$ are evaluated, the quotient is the 'modulator' giving the real time value of the drift force. The long term average (say 0.5 hour) of the 'modulator' is 1.

The subscript j = 1, 2 stands for the components in x and y direction with respect to the ship. The moment component in the horizontal plane (ψ) cannot be directly determined in this approach of Method 2 because of lack of information. For, the moment on the ship changes sign if a wave group passes midship. A simplified estimate is used, by using the computations to associate to each combination of T_{zus} and α_r a point of application of F_y with respect to the midships, x_{Fy} , and then use the estimate:

$$M_z(t) \cong x_{Fy} \,.\, F_2 \qquad (9)$$

as wave drift moment acting on the vessel.

In this computation the wave direction is needed to solve Eq. (7). The wave direction α_{rel} follows from the relative motion measurements at the sides according to the method of Aalbers and Nienhuis (Ref. 9), described in short below.

Wave direction estimator

The wave direction with respect to the vessel can be estimated from the difference in the relative motion at windward side and lee side. For the vessel under consideration the measurement locations at the forward shoulders showed to give the most consistent and distinct difference between windward and lee side relative motions.

The ration between the two is defined as:

$R(\alpha_{rel}) = \int S_{s\text{-}PS}(\omega)d\omega \,/\, \int S_{s\text{-}SB}(\omega)d\omega$ for wave directions approaching from Port (PS)
and
$R(\alpha_{rel}) = \int S_{s\text{-}SB}(\omega)d\omega \,/\, \int S_{s\text{-}PS}(\omega)d\omega$ for wave directions approaching from Starboard (SB) (10)

The graph in Fig. 6 shows the ration as a function of wave direction for a range of wave spectra with average wave periods covering the operational sea states ($5 < T_z < 10$ s). The error margins in the graph indicate the standard deviation of the mean ration value for those spectra.
This standard deviation is small so that a reasonable accuracy of the wave direction estimate may be expected.

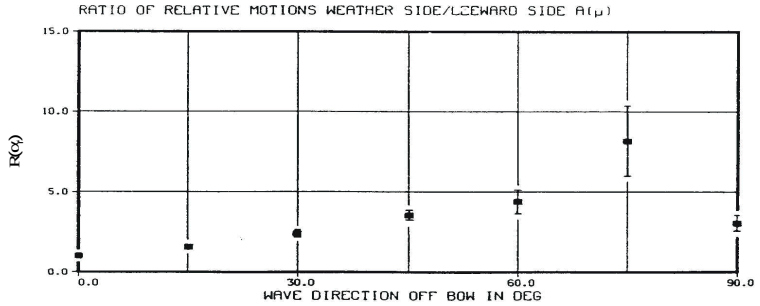

Fig. 6: Dependence on wave direction of relative motion ratio between Port and Starboard side

3.3 DP model test

The model tests were carried out using a tanker hull form at scale 1 to 50, equipped with a single, large size azimuthing thruster at the bow and at the stern. Each model thruster represented a combination of several thrusters in reality. The relative wave height sensor positions on the model are shown in Figure 7, where all positions were used for Method 1 and the numbers 1, 5 and 6 for the Method 2. (Note: the numbering corresponds to the positions defined for the numerical preparation work).

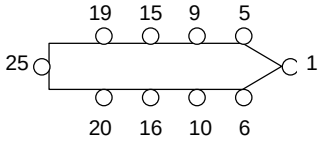

Fig. 7: Schematic positions of relative motion probes on model.

The dynamic positioning system in the basin (RUNSIM) uses a low frequency Kalman filter for low frequency position control, described by Nienhuis et al (Ref. 11). The control loop has the following main components:

- Low frequency extended Kalman Filter
- Feed-back position control module on basis of PID coefficients
- Optimum power thrust allocation
- Wave drift force feed forward

Although it would have been quite feasible with the available information from the feed forward module, there was no automatic heading optimization implemented. The reason therefore was that a straight comparison of DP performance on the same heading setpoint could be made between conventional and feed forward control.

Feed Forward Control

The external forces acting on a dynamically positioned vessel at sea are caused by:

- current
- waves
- wind
- thrusters
- hydrodynamic reaction forces

When the ship stays on the same position the sum of all forces equals 0. So, the basic assumption is:

$$\overline{F_{thr}} = -\{\overline{F_{win}} + \overline{F_{wav}} + \overline{F_{cur}} + \overline{F_{reac}}\} \qquad (11)$$

In conventional DP control systems the current and wave forces (F_{cur} and F_{wav}) are not known. The required thruster force (F_{thr}) is known from the allocation algorithm and the wind force (F_{win}) can be estimated from the measured wind speed and direction (Wind Feed Forward). Therefore F_{cur} and F_{wav} are estimated jointly as the so-called 'rest force':

$$\overline{F_{wav} + F_{cur}} = -\{\overline{F_{thr}} + \overline{F_{reac}} + \overline{F_{win}}\} \qquad (12)$$

In Wave Drift Force Feed Forward DP control, with the wave drift force estimate available according to Section 2, the Eq. (11) can be further elaborated. It is possible to take out the quite strongly varying external force F_{wav} . Hence, the remaining estimate for the very slowly varying current force is:

$$\overline{F_{cur}} = -\{\overline{F_{wav}} + \overline{F_{thr}} + \overline{F_{reac}} + \overline{F_{win}}\} \qquad (13)$$

Furthermore, the wave drift force estimate is used directly in the PID feed back loop by adding the forces F_x , F_y and M_z to the required positioning forces from the PID controller.

The wave conditions during the tests represent Pierson Moskowitz type irregular sea spectra. The setup allows to also test in cross seas, utilizing wave generators at two sides of the basin to make a typical wind sea and a swell. Sea states between 2 m and 10 m significant were generated for the model tests.
The test duration corresponded to 1 hour full scale, and the measurements were statistically analyzed. Furthermore, time traces and position plots were made for presentation of the results.

Discussion of the results

In Figures 8 [a and b] the time traces of a representative part of the tests in a Beaufort 9 Condition are shown.

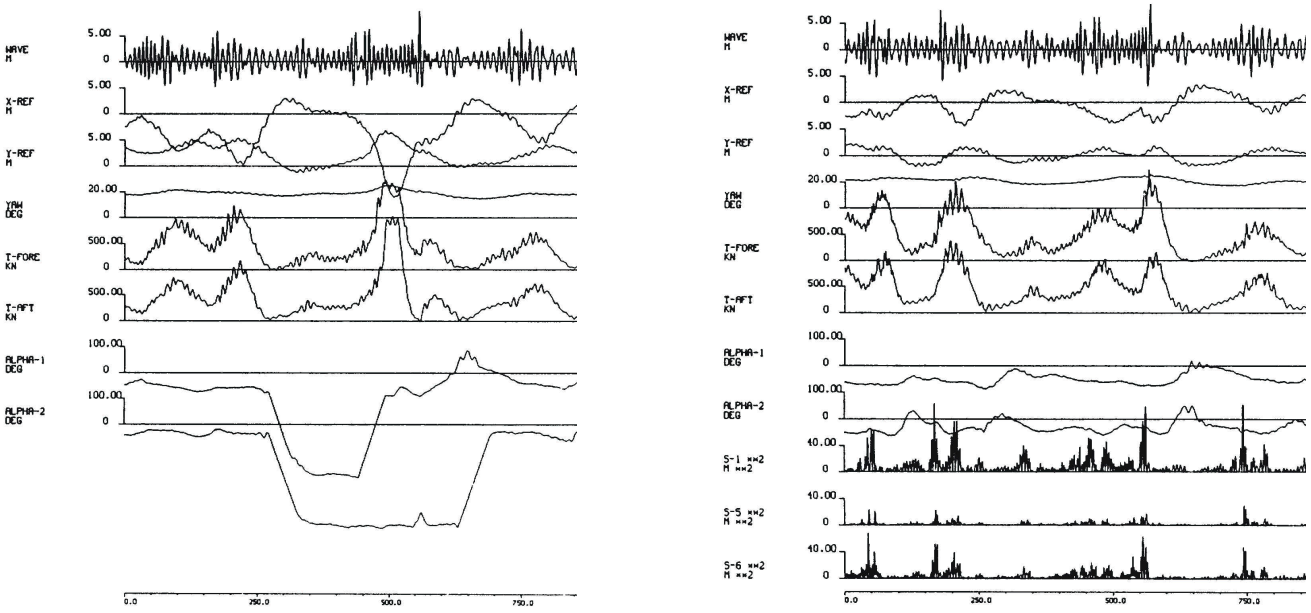

Fig. 8[a and b]: Measured time traces of model test with and without wave feed forward using method 2.

The results of the tests give as general conclusion that the use of Wave feed Forward improves the position standard deviations significantly for virtually the same thrust. The largest improvements were found in the X motion while for sway (Y) and yaw the improvements were minor. This can be explained from analysis of the Wave Feed Forward estimate methods.

The drift moment estimate is important for sway and yaw. The simplification of Eq. 9 ignores the fact that when a wave group passes the ship, the drift moment exerted on the vessel will change sign when the group passes the midship. The Y-force keeps the same sign and so does the estimate for the moment from Eq. 9.
The Y-force estimate is sensitive to the wave direction estimate from the relative motion sensors on the starboard and port side shoulder. In Table 3 the results are given of the wave direction estimates for several tests and compared with the actually measured values. The comparison shows that the direction estimate is surprisingly good. If for the cross-sea an energy averaged wave direction is calculated, viz. 202.1 deg, the result is also good.

Table 3

Test No.	Condition	Estimated wave direction		Measured wave direction	
		Mean	Standard dev.	Mean	Standard dev
24501	1	188.4	0.30	180	1.31
23702	4	179.2	0.99	180	0.98
249301	5	197.6	0.88	cross sea	1.24
23201	6	185.6	0.52	180	1.98
25201	8	184.7	0.33	180	4.64
25501	9	183.6	0.18	180	2.14

A shortcoming of the wave direction estimating method is that for wave directions more or less beam on to the vessel the function $R(\alpha)$ of Figure 5 may give an undefined solution. On the other hand it must be realised that the wave drift forces for wave directions around beam on are quite similar in magnitude. So, the error in wave direction does not necessarily lead to serious errors in the drift force estimates.

4. CONCLUSIONS

Hydrodynamic investigations and model tests can provide useful information on the stationkeeping performance of dynamically positioned vessels. Complex phenomena like the wave drift forces on the vessel, as well as thruster-current, thruster-hull, thruster-thruster and thruster-wave interactions are quantified, so that they can be accounted for in design. Furthermore, full DP model tests offer the possibility to investigate the effect of different control settings, thrust allocation methods and feed forward. A DP control method with wave drift force feed forward was experimentally tested and a number of conclusions could be drawn:

- The application of wave feed forward leads to improved positioning for the same power.
- The method used to estimate the (average) wave direction is good
- Further developments are needed to improve the wave drift force estimation and to allow the method 2 to be used for all ship headings.

REFERENCES

1. Nienhuis, U., “Analysis of Thruster Effectivity for Dynamic Positioning and Low Speed Maneuvering,” PhD thesis Delft University of Technology, Delft (October 1992).
2. Minsaas & Lehn: “Hydrodynamic characteristics of rotatable thrusters.”. NTFI Report 69-78, 1978
3. Brix, J.: “Querstrahlsteuer,” Forschungzentrum des Deutschen Schiffbaus, Bericht No 80, 1978
4. J.L. Cozijn, B. Buchner, R.R.T. van Dijk, MARIN, “Hydrodynamic Research Topics for DP Semi Submersibles,” OTC 10955, Houston, May 1999.
5. D. Deter and H. Shatto: “Interaction Between Thrusters, Power Systems and DP Control Systems.” MTS DP Conference, Houston, 1999.
6. A.B. Aalbers, R.B.H.J. Jansen, R.J.P.E. Kuiper and Van Walree, F.: “Developments in dynamic positioning systems for offshore station keeping and offloading.” ISOPE The Hague, June 1995
7. J.A. Pinkster, “Low Frequency Second Order Wave Exciting Forces on Floating structures”, Thesis, Delft University of Technology, 1980.
8. J.A. Pinkster, “Wave-feed-forward as a Means to improve dynamic positioning”, OTC 3057, Houston, 1978
9. A.B. Aalbers and U. Nienhuis, “Wave direction Feed-forward on Basis of Relative Motion Measurements to Improve Dynamic Positioning Performance”, OTC 5445, Houston, 1987.
10. A.B. Aalbers, R.P. Tap, J.A. Pinkster: “An Application of wave feed forward to dynamic positioning control,” IFAC Journal on Applied Non-linear Control. J. Wiley, New York, to be published November 2001
11. U. Nienhuis, H.J.M. de Bock and P.H. Braker, “Simulations of DP vessels by Model Tests of Computations,” Maritime Research Institute Netherlands, September 1987.